Fault prognosis feature extraction and selection for bearings based on statistical indicator optimization

Tan Xiaodong[1,2]

1. School of Mechanical and Electrical Engineering
University of Electronic Science and Technology of China
Chengdu, China
xdt1010@126.com

2. Department of Force Management
Officers College of PAP
Chengdu, China

***Abstract*—Fault evolution feature extraction is the key to tracking and monitoring fault development, and triggering prognosis and health management. However, traditional time-frequency domain methods didn't consider the effectiveness of features for the whole lifecycle process, and it supports a low degree for fault prognosis and health state assessment. A fault prognosis feature extraction method based on statistical indicator optimization selection is proposed in this paper. Firstly, original signals of bearings in the whole lifecycle are collected, then their statistical indicators at each echo are calculated, thus those fault evolution trend curves described by all statistical indicators will be generated. Secondly, fault trend analysis is implemented based on the above fault evolution curves, then the monotonicity, trendability, identifiability and robustness of all features for fault evolution curves can be calculated. Thirdly, the monotonicity, trendability, identifiability and robustness of each feature are translated into a hybrid metric, and those hybrid metrics of all features are sorted by size, thus the fault prognosis features will be selected appropriately. Finally, the life-time data of bearings provided by University of Cincinnati are used to verify the effectiveness of the proposed method in this paper.**

Keywords- Bearings; Feature extraction; Prognosis and health management; Statistical indicator optimization

I. INTRODUCTION

Bearings are important components in rotatory mechanical systems, but due to the effect of high load, high impact, complicated work condition, failure happens frequently in the inner race, outer race and the rolling parts. If an effective fault detection method is not taken, the bearing will result in functional failure with the development of incipient fault, and it will lead to the loss of properties and lives[1]. So, tracking and monitoring the development and evolution of a fault can provide lots of useful information for fault prognosis and health state assessment. It is essential to trigger the health management mechanism in order to improve operational efficiency and reduce the risk due to sudden functional failure. However, the abnormal signals of faulty bearings present nonlinearity and nonstationarity, which brings potential difficulties in the fault prognosis[2]. The weak signals in the powerful chaos and noise with great stability and reliability can not be detected in time. Meanwhile, fault prognosis pays more attention to the features which can describe the fault evolution process. So, it is a key to tracking the fault development by extracting fault prognosis features under strong noisy environment [3,4].

Recently, advanced signal processing technology has received considerable attentions and has made remarkable achievements in the field of fault diagnosis, prognosis and condition monitoring for bearings[5,6]. Li et al., Zhong et al., Wang, and He et al., proposed some methods to extract fault signatures for the early failure stage of bearings [7-9]. Javed et al. defined a predictable feature to get better RUL estimation[10]. Tan et al., and Lei et al., used a series of statistical indices to monitor the development of mechanical faults and provided available information for fault prognosis[1,4]. The vibration signals of mechanical components are usually corrupted by strong noise in the whole lifecycle process, and the ability to describe the fault growth process differs among various statistical indicators. So the optimal faulty features in the fault development stage are of great importance, and those features should present more power during the whole fault growth period. In the light of the success in economic prediction, weather forecast and military prediction through big data mining and statistical analysis, a fault evolution characteristic analysis and feature extraction and selection based on statistical indicator optimization is proposed in this paper. Firstly, life-time data of bearings in the whole lifecycle are collected, then statistical indicators of original vibration data at each echo are calculated, thus those fault evolution curves described by all indicators will be created. Secondly, the monotonicity, trendability, identifiability and robustness of all features for fault evolution trends can be calculated. Thirdly, the four abilities of each feature are translated into a comprehensive index, and those indices are sorted by size, thus the fault prognosis features will be selected appropriately. Finally, the life-time data of bearings provided by University of Cincinnati are used to verify the effectiveness of proposed methods in this paper.

II. STATISTICAL INDICATOR OPTIMIZATION

A. *Computational formulas*

Bearing faults belong to the soft fault, which usually go through a process of slow change. It is therefore that a significant feature should focus on the overall fault growth process. Statistical indices that are effective in describing a trend, such as RMS and kurtosis, have been considered here.

*Corresponding author: Tan Xiaodong
Tel.: +86-13980979642.
E-mail address:xdt1010@126.com
Foundation item: National Natural Science Foundation (61403408)
978-1-7281-0860-5/19/$31.00 ©2019 IEEE

Higher order statistics in frequency-domain can also be extracted as possible prognosis features for fault growth process which are often nonlinear and nonstationary [4]. In this paper, some statistical indicators in time and frequency domain for monitoring fault evolution process and their calculating equations are tabulated in Tab. I [1,11-13].

TABLE I. Statistical indicators in time and frequency domain

Serial number	**Calculation formula**	**Serial number**	**Calculation formula**	**Serial number**	**Calculation formula**
F_1	$\frac{\sum_{n=1}^{N} x(n)}{N}$	F_2	$\sqrt{\frac{\sum_{n=1}^{N}\left[x(n)_1\right]^2}{N}}$	F_3	$\left(\frac{\sum_{n=1}^{N}\sqrt{\lvert x(n)\rvert}}{N}\right)^2$
F_4	$\frac{\sum_{n=1}^{N}\lvert x(n)\rvert}{N}$	F_5	$\frac{\sum_{n=1}^{N}\left[x(n)\right]^3}{N}$	F_6	$\frac{\sum_{n=1}^{N}\left[x(n)\right]^4}{N}$
F_7	$F_7=\frac{\sum_{n=1}^{N}\left[x(n)-F_1\right]^2}{N-1}$	F_8	$F_8=\max\lvert x(n)\rvert$	F_9	$\sqrt{\frac{\sum_{n=1}^{N}\left[x(n)-F_1\right]^2}{N-1}}$
F_{10}	F_8-F_9	F_{11}	$\frac{\sum_{n=1}^{N} x^2(n)}{N}$	F_{12}	$\frac{F_2}{F_4}$
F_{13}	$\frac{F_8}{F_2}$	F_{14}	$\frac{F_8}{F_4}$	F_{15}	$\frac{F_8}{F_3}$
F_{16}	$\frac{F_5}{(F_7)^{\frac{3}{2}}}$	F_{17}	$\frac{F_6}{(F_7)^2}$	F_{18}	$\frac{\sum_{k=1}^{N_{FT}} S(k)}{N_{FT}}$
F_{19}	$\frac{\sum_{k=1}^{N_{FT}}\left(S(k)-F_{18}\right)^2}{N_{FT}-1}$	F_{20}	$\frac{\sum_{k=1}^{N_{FT}}\left(S(k)-F_{18}\right)^2}{N_{FT}\left(F_{19}\right)^{\frac{3}{2}}}$	F_{21}	$\frac{\sum_{k=1}^{N_{FT}}\left(S(k)-F_{18}\right)^4}{N_{FT}\left(F_{19}\right)^2}$
F_{22}	$\frac{\sum_{k=1}^{N_{FT}} f_k S(k)}{\sum_{k=1}^{N_{FT}} S(k)}$	F_{23}	$\sqrt{\frac{\sum_{k=1}^{N_{FT}}\left(f_k-F_{22}\right)^2 S(k)}{N_{FT}}}$	F_{24}	$\sqrt{\frac{\sum_{k=1}^{N_{FT}} f_k^2 S(k)}{\sum_{k=1}^{N_{FT}} S(k)}}$
F_{25}	$\sqrt{\frac{\sum_{k=1}^{N_{FT}} f_k^4 S(k)}{\sum_{k=1}^{N_{FT}} f_k^2 S(k)}}$	F_{26}	$\frac{\sum_{k=1}^{N_{FT}} f_k^2 S(k)}{\sqrt{\sum_{k=1}^{N_{FT}} S(k)\sum_{k=1}^{N_{FT}} f_k^4 S(k)}}$	F_{27}	$\frac{F_{23}}{F_{22}}$
F_{28}	$\frac{\sum_{f=1}^{N_{FT}}\left(f_k-F_{22}\right)^3 S(k)}{N_{FT}F_{23}^3}$	F_{29}	$\frac{\sum_{k=1}^{N_{FT}}\left(f_k-F_{22}\right)^4 S(k)}{N_{FT}F_{23}^4}$	F_{30}	$\frac{\sum_{k=1}^{N_{FT}}\sqrt{\lvert f_k-F_{22}\rvert}S(k)}{N_{FT}\sqrt{F_{23}}}$

where, $x(n)$ is a raw experimental vibration signal, $S(k)$ is the frequency spectrum of $x(n)$, N_F is the number of spectrum lines, f_k is the frequency value of kth spectrum line.

B. The abilities to track fault growth process

Actually, detecting the incipient fault and tracking the fault growth process directly affect the precision and validation of fault prognosis. Thus, a fault feature should contain abundance of fault growth information in order to detect the incipient fault as early as possible and effectively track the fault growth process. However, not all of the extracted features are necessarily useful. Thus the primary task of fault feature extraction for fault prognosis is to quantify the abilities of all sorts of features to detect the incipient fault and track the fault growth process. In order to assess the ability of a feature to monitor and track the fault growth process, the monotonicity, trendability, identifiability and robustness of features are used and the calculation functions are presented in Eqs(1)-(4)[4].

$$\phi_1(X)=\frac{1}{K-1}\left|No.of\left(d/dx>0\right)-No.of\left(d/dx<0\right)\right| \quad (1)$$

where, $\phi_1(X)$ is used to assess the consistently increasing or decreasing trend of a feature, $X=\{x_k\}_{k=1:K}$ is the time series to describe the fault evolution trend, x_k is the time value of X, K is the number of statistical features, $d/dx=x_k-x_{k-1}$, $No.of(d/dx>0)$ is the number of $(d/dx>0)$, and $No.of(d/dx<0)$ is the number of $(d/dx<0)$.

$$\phi_2(X,T)=\frac{K\left(\sum_{k=1}^{K}x_k t_k\right)-\left(\sum_{k=1}^{K}x_k\right)\left(\sum_{k=1}^{K}t_k\right)}{\sqrt{\left[K\left(\sum_{k=1}^{K}x_k^2\right)-\left(\sum_{k=1}^{K}x_k\right)^2\right]\left[K\left(\sum_{k=1}^{K}t_k^2\right)-\left(\sum_{k=1}^{K}t_k\right)^2\right]}} \quad (2)$$

where, $\phi_2(X,T)$ is defined as the trendability to monitor the whole fault evolution process, t_k is the k th value of the time and x_k is the feature value at t_k, $\phi_2(X,T)$ changes from -1 to 1, and $\phi_2(X,T)=1$ or $\phi_2(X,T)=-1$ means that features have a strong positive or negative linear correlation with time.

$$\phi_3(X,C)=\sum_{s=1}^{S}\sum_{d\neq s}^{S}\frac{\left(m_s-m_d\right)^2}{\sigma_s^2+\sigma_d^2} \quad (3)$$

where, $\phi_3(X,C)$ is defined as the ability to diagnose various fault types with different statistical features. S is the number of fault types, m_s and σ_s^2 are the mean values and the variances with sth fault state, respectively. The higher the value is, the more effective to identify different fault states the feature is in.

$$\phi_4(X)=\frac{1}{K}\sum_{k=1}^{K}\exp\left(-\left|\frac{x_k-x_k^T}{x_k}\right|\right) \quad (4)$$

where, $\phi_4(X)$ is defined as the stability of the prediction results to track a fault trend with the measurement noise, stochasticity of the degradation processes and the variation of operational conditions, x_k is the feature value of X at t_k, and x_k^T is the mean trend value of the feature at tk which is generally acquired through smoothing methods. Robustness reflects the tolerance of the feature to outliers. In order to formulate a weighted linear combination of the proposed metrics as the degradation feature selection criteria, a comprehensive index is proposed.

$$\Phi=\omega_1\phi_1(x)+\omega_2\phi_2(X,T)+\omega_3\phi_3(X)+\omega_4\phi_4(X) \quad (5)$$

where Φ is the objective function to be optimized, and ω_i is the significance put on the individual metric.

III. FAULT PROGNOSIS FEATURE EXTRACTION

Finally, complete content and organizational editing before formatting. Please take note of the following items when proofreading spelling and grammar:

The flow of fault trend analysis and prognosis feature extraction is shown in Fig. 1. It includes data acquisition and preprocessing, the calculation of time-frequency statistical indicators of original signals, fault trend analysis and prognosis feature extraction and so on.

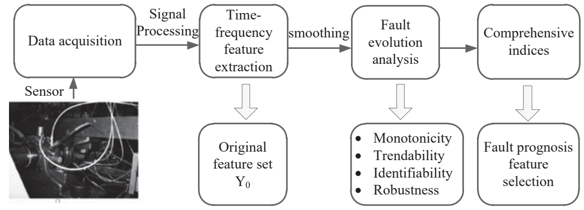

Figure 1. The flow of fault feature extraction and selection

Collecting the complete life test data and make data set have some independent characteristics and remove noise from data.

Calculating the statistical indicators by using the above methods introduced in section 1.1, and creating the fault evolution curves.

Analyzing the mononicity, trendability, identifiability and robustness of each statistical indicator using Eqs(1)-(4), respectively.

Computing the comprehensive index Φ for each feature using Eq.(5), and the fault prognosis features are selected according to the result of Φ.

IV. CASE STUDIES

The openly available data provided by Intelligent Maintenance System, University of Cincinnati are used to test the validity of the method proposed in this paper [7,14]. The bearing test experimental system is shown in Fig.2. The major parameters of experimental bearings are listed in Tab.II, as shown in TABLE II. Each bearing has 16 rollers in each row, a pitch diameter of 2.815 inches, roller diameter of 0.331 in., and a tapered contact angle of 15.17◦. On each bearing, two PCB 353B33 High Sensitivity Quartz ICP accelerometers are installed for data acquisition (one vertical and one horizontal) as shown in Figure 2. Meanwhile, the vibration signals are measured at an interval of every 10 min. Besides, the sampling frequency is 20000 Hz and the data length is 20480 points. The shaft rotating speed of the motor is 2000 rpm. At the end of the accelerated experiment, an outer race fault is discovered in test bearing 1 and 984 files are collected (Total running time is 9840 minutes). More detailed information about this experiment is shown in literature [7].

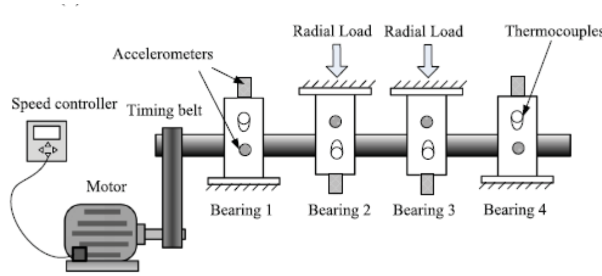

Figure 2. Bearing fault test platform

TABLE II. The major parameters of experimental bearings

Bearing specification	**Rows of rollers**	**The number of rollers in each row**
ZA-2115	2	16
Inner diameter	Roller diameter	Contact angle
71.5mm	8.5mm	15.17°

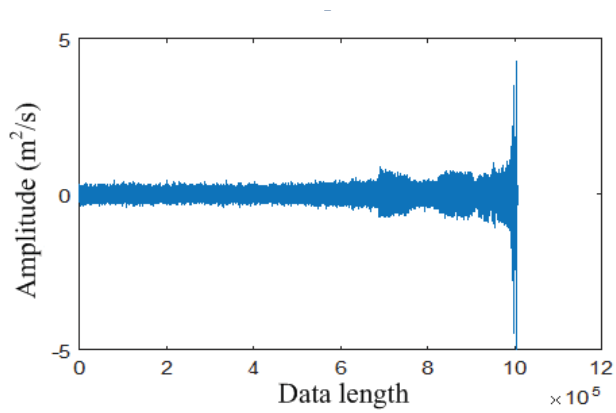

Figure 3. Original waveforms in the whole lifecycle

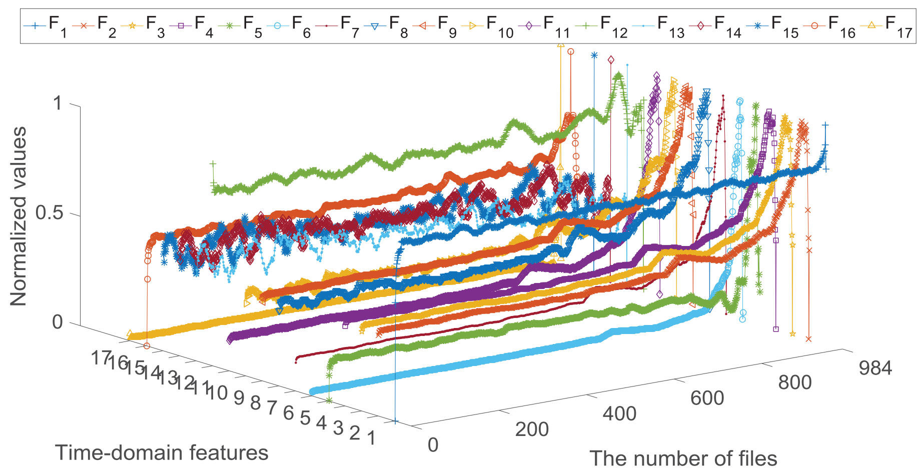

Figure 4. Fault growth trend curves of time-domain features

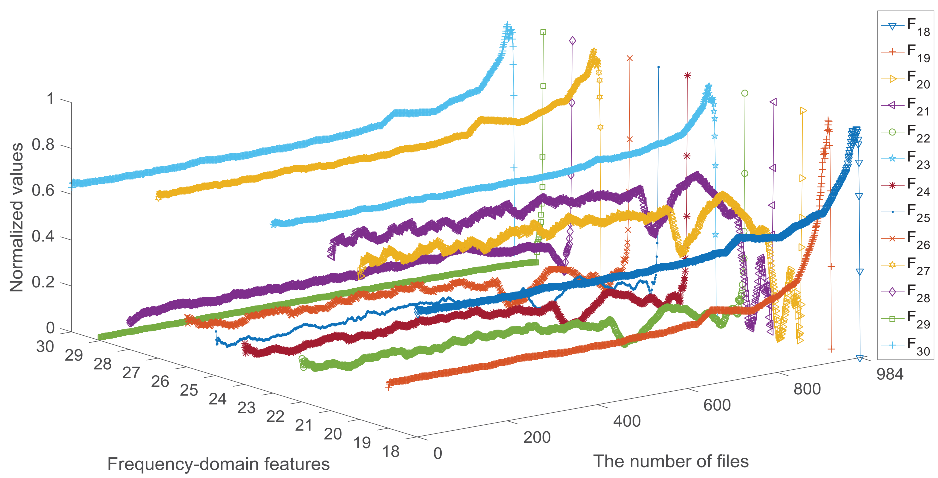

Figure 5. Fault growth trend curves of frequency-domain features

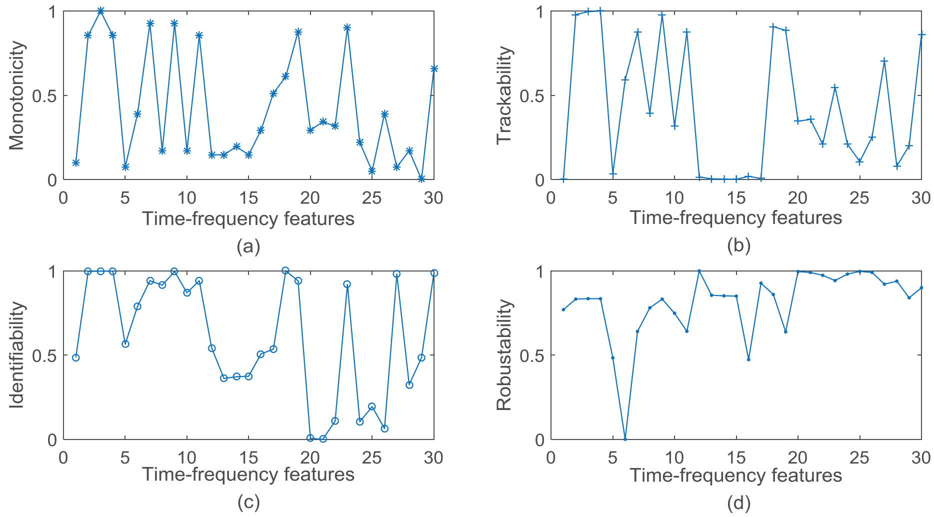

Figure 6. The comparisons of four abilities of 30 features to track fault growth process

Original waveforms in the whole lifecycle are shown in Fig. 3, and it suggests that the vibration amplitudes increase gradually with fault growth. Especially at the end of failure, the value grows suddenly. According to the mathematical formulas of statistical indices introduced in Tab. I, the feature of each data file in lifecycle time can be calculated, then the fault evolution trend curves described by those features can be created. The time-domain and frequency-domain statistical indices are shown in Fig. 4 and Fig. 5, respectively. Fig. 5 shows that the trend of feature F_3 (RMS) is stable in the whole life cycle, but there is a sudden increase at the end of bearing failure, which means that RMS can not be used to find incipient weak fault symptom but can effectively describe the whole fault growth process. Peak values increase gradually at the incipient fault stage, but fluctuate in the whole lifecycle of bearings, and don't show the specific amplitude. Impulsion index and tolerance index of the vibration signal change faintly at the early fault stage, and they do not have an obvious trend, while they increase distinctly at the end of bearing failure, and they are not sensitive for the sudden failure. Kurtosis index changes steadily at the early stage, but it presents more sensitivity to the failure stage.

In order to quantify the abilities of 30 statistical indices to track fault growth process, the above abilities can be calculated by Eqs(1)-(4), respectively, and they are normalized. The comparison result is shown in Fig. 6. The comprehensive indices of all features to track the fault growth process are calculated by Eq.(5), and the calculation results are listed in Tab. III. The results show that the comprehensive indices of features F_3, F_2, F_4 and F_9 are greater than 0.9, and the comprehensive indices of F_7,F_{11},F_{18},F_{19},F_{23},F_{30} are confined to 0.8-0.9.

TABLE III. Comprehensive indices of 30 features

Features	F_1	F_2	F_3	F_4	F_5	F_6	F_7	F_8	F_9	F_{10}	F_{11}	F_{12}	F_{13}	F_{14}	F_{15}
$\boldsymbol{\Phi}$	0.34	**0.92**	**0.96**	**0.92**	0.29	0.44	**0.85**	0.57	**0.93**	0.53	**0.83**	0.43	0.34	0.36	0.34
Features	F_{16}	F_{17}	F_{18}	F_{19}	F_{20}	F_{21}	F_{22}	F_{23}	F_{24}	F_{25}	F_{26}	F_{27}	F_{28}	F_{29}	F_{30}
$\boldsymbol{\Phi}$	0.32	0.50	**0.84**	**0.84**	0.41	0.42	0.40	**0.83**	0.38	0.34	0.42	0.67	0.38	0.38	**0.85**

TABLE IV. The prognosis error for those features whose comprehensive indices are greater than 0.8

Features	**Comprehensive indexes**	**Exponential Smoothing Estimation Method**	**Logistic prediction**	**GRNN**
F_2	0.92	0.1926	0.1945	0.1927
F_3	0.96	0.2084	0.1986	0.1944
F_4	0.92	0.2040	0.2011	0.1936
F_7	0.85	0.2437	0.2678	0.2139
F_9	0.93	0.1930	0.2036	0.1938
F_{11}	0.83	0.2437	0.2987	0.3145
F_{18}	0.84	0.2368	0.2685	0.2906
F_{19}	0.84	0.2405	0.2784	0.3011
F_{23}	0.83	0.2422	0.2901	0.3126
F_{30}	0.85	0.2869	0.2763	0.2984

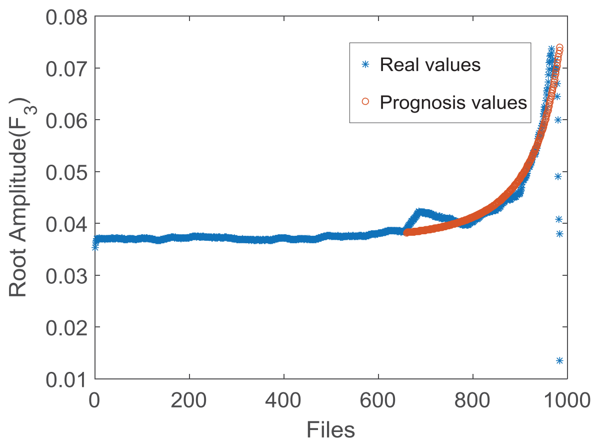

Figure 7. The prognosis curve of fault evolution trend for F_3

In order to compare the prognosis error for each feature, exponential smoothing, Logic return model and Generalized Regression Neural Network (GRNN) are used to predict the time to failure from 650th files , and the fault prognosis curves using F_3 are shown in Fig. 7. Due to space limitations, Tab. IV only presents the prognosis errors whose comprehensive indices are greater than 0.8. As shown in Tab. IV, it can be seen that the errors among F_2, F_4 and F_9 are smaller than other 27 features, because their comprehensive indices are greater 0.9. Above all, the bigger the comprehensive index, the smaller the prognosis error is. Therefore, the results show that the proposed method in this paper can provide an effective way to select more robust, sensitive and monotonic features for fault prognosis.

V. Conclusion

Statistical indicator optimization is helpful to expand the potential laws of fault development and evolution hidden behind a lot of background noise, and those statistical features can effectively describe the fault evolution trend although their fault prognosis result has a remarkable distinction among various features. The monotonicity, trendability, identificability and robustness can describe accurately the ability of a fault feature to track and monitor the fault evolution process. According to the experiments, root amplitude, standard deviation, RMS, absolute value, variance and average power have good monotonicity, strong robustness and fault identifiability to monitor the fault evolution process compared to the other indicators, and those features can provide abundance of useful information for fault prognosis.

Also it needs to be stressed that the proposed method in this paper is universally applicable to further study of the wheel gear, shaft, and so on, and the differences lie in the fault types and components. So, the future work will cover its fault types to rolling and inner race faults, and the subjects of study can extend to the wheel gears and shafts.

Acknowledgment

This research is partially supported by the National Natural Science Foundation of China under contract number 61403408. We will appreciate deeply the members of the Laboratory of Science and Technology on Integrated Logistics Support at the National University of Defense Technology and Officers College of PAP.

References

[1] X. D. Tan, J. Qiu, Y. Zhang et al, “Feature Extraction Technique for Fault Prognosis Based on Fault Trend Analysis,” Journal of Donghua university, vol.34, no.6, pp.784-787, 2017.

[2] F. Yang, M.S.Habibullah, T. Zhang et al, “Health index-based prognostics for remaining useful life predictions in electrical machines,”. IEEE transaction Industry Electronic, vol. 63, pp. 2633-2644, 2016

[3] Y. G. Lei, N. Li, J. Gontarz et al, “A model-based method for remaining useful life prediction of machinery,” IEEE Transaction Reliability, vol. 65, pp.1314-1326, 2016.

[4] Y. G. Lei, N.P. Li, L. Guo et al, “Machinery health prognostics: A systematic review from data acquisition to RUL prediction,” Mechanical systems and signal processing, vol. 104, pp.799-834, 2018.

[5] G.J.Tang and X.L.Wang, “Adaptive maximum correlated Kurtosis deconvolution method and its application on incipient fault diagnosis of bearing ,” Proceedings of the CSEE, vol.35, no.6, pp.1436-1444, 2015.

[6] X. M. Sun, H. Liu, X.G. Zhao et al, “Singular Point Recognition and Feature Extraction for Incipient Bearing Fault Based on Instantaneous Envelope Scalogram Entropy,” Journal of mechanical engineering, vol. 53, no.3, pp.73-80, 2017.

[7] Y. B. Li, X. H. Liangb, M.Q. Xua et al, “ Early fault feature extraction of rolling bearing based on ICD and tunable Q-factor wavelet transform,” Mechanical Systems and Signal Processing, vol.86, pp. 204-223, 2017.

[8] Z.H. Wang, X. Wu, X.Q. Liu et al, “Research on feature extraction algorithm of rolling bearing fatigue evolution stage based on acoustic emission,” Mechanical Systems and Signal Processing, vol.113, pp.271-284, 2018.

[9] G. L. He, K Ding, H.B. Lin, “Fault feature extraction of rolling element bearings using spare representation,” Journal of sound and vibration, vol. 366, pp.514-527, 2016.

[10] K. Javed, R. Gouriveau, P. Zerhouni et al, “Enabling health monitoring approach based on vibration data for accurate prognostics,” IEEE Transaction Industry Electronics, vol.62, pp.647-656, 2015.

[11] J. H. Liu, X. M. Dong, J.F. Li, “Fault feature extraction of rolling bearings based on noises reduced by full vector spectrum ITD_ICA Blind source separation,” China Mechanical Engineering, vol.29, no.8, pp.943-948, 2018.

[12] A. Rai, S. Upadhyay, “A review on signal processing techniques utilized in the fault diagnosis of rolling element bearings,” Tribology International, vol. 96, pp.289-306, 2016.

[13] B. Zhang, L. Zhang, J. Xu et al, “Degradation feature selection for remaining useful life prediction of rolling element bearing,” Quality Reliability Engineering International, vol.32, pp.547-554, 2015.

[14] H. Qiu, J. Lee, J. Lin et al, “Wavelet filter-based weak signature detection method and its application on rolling element bearing prognostics,” Journal of Sound and Vibration, vol.289, pp.1066-1090, 2006.